Atmos. Chem. Phys. Discuss., 15, 24403–24417, 2015
www.atmos-chem-phys-discuss.net/15/24403/2015/
doi:10.5194/acpd-15-24403-2015

Atmospheric Chemistry and Physics
Discussions
Open Access

The latitudinal structure of recent changes in the boreal Brewer–Dobson circulation

C. Shi[1,2], D. Guo[1,2], J. Xu[2], A. M. Powell Jr.[3], and T. Xu[1]

[1]Key Laboratory of Meteorological Disaster of Ministry of Education, Nanjing University of Information Science and Technology, Nanjing, Jiangsu, China
[2]GENRI, College of Science, George Mason University, Fairfax, VA, USA
[3]NOAA/NESDIS/STAR, College Park, MD, USA

Received: 22 July 2015 – Accepted: 20 August 2015 – Published: 8 September 2015

Correspondence to: C. Shi (shich1997@gmail.com) and J. Xu (jxu14@gmu.edu)

Published by Copernicus Publications on behalf of the European Geosciences Union.

The latitudinal structure of recent changes in the boreal Brewer–Dobson circulation

C. Shi et al.

Abstract

Upwelling branch of the Brewer–Dobson circulation (BDC) controls the tropical lower stratospheric water vapor (WV) through dynamic cooling near the tropopause. Downwelling branch of BDC dominates the extratropical middle-lower stratospheric Hydrogen Chloride (HCl) by dynamic transport. Climatologically, a symmetric weakening BDC indicates increasing tropical lower stratospheric WV and decreasing extratropical middle-lower stratospheric HCl. However, the global ozone chemistry and related trace gas data records for the stratosphere data (GOZCARDS) show that the tropical lowermost stratospheric WV increased by 18 % decade^{-1} during 2001–2011 and the boreal mid-latitude lower stratospheric HCl rose 25 % decade^{-1} after 2006. We interpret this as resulting from a slowdown of the tropical upwelling and a speedup of the mid-latitude downwelling. This interpretation is supported by composite analysis of Eliasen–Palm Flux (EPF), zonal wind and regression of temperature on the EPF from the ERA-Interim data. Results present that the enhancing polar vortex and weakening planetary wave activity leads to a downwelling branch narrowing equatorward and a local speedup of 24 % at 20 hPa in the mid-latitudes. Moreover, there are regressive temperature increase of 1.5 K near the tropical tropopause and that of 0.5 K in the mid-latitude middle stratosphere, which also indicates the tropical upwelling slowdown and the mid-latitude downwelling speedup during 2001–2011.

1 Introduction

It has recently been discovered that the stratospheric trace gases, such as Water Vapor (WV) and Hydrogen Chloride (HCl), tend to have anomalous trends since the beginning of the 21st century (Mahieu et al., 2014; Fueglistaler, 2012). Solomon et al. (2010) suggested that decrease of the lower stratospheric WV leads to a 25 % reduction of the global warming rate near 2000, which indicates that WV plays an important role in the balance of the global radiation. Mote et al. (1995) detected the “tape recorder”

ACPD
15, 24403–24417, 2015

The latitudinal structure of recent changes in the boreal Brewer–Dobson circulation

C. Shi et al.

effect on tropical WV above the tropopause and pointed out that the WV variability is dominated by dehydration based on the tropical Cold-Point Tropopause Temperature (CPTT). The tropical CPTT is connected with dynamic cooling of upwelling branch of Brewer–Dobson circulation (BDC). In addition, in December, January, February and March (DJFM), a large proportion of WV transport into stratosphere over the Tropical Western Pacific (TWP) is known as "stratospheric fountain" (Geller et al., 2002; Bannister et al., 2004; Bonazzola et al., 2004). Thus, the variability of the BDC in the boreal winter affects the annual tropical lower stratospheric WV (Dessler et al., 2014).

The principal source for Stratospheric HCl is the decomposition of chlorofluorocarbons (CFCs) in the upper stratosphere under intense ultraviolet radiation (UV). HCl is relatively long-lived in the stratosphere (Mohanakumar, 2008; Andrews et al., 1987) and is transported downward by the downwelling branch of deep BDC. Due to the Montreal Protocol, the total atmospheric chlorine of CFCs decreased since 1992/93 and stratospheric HCl declined after 1997 as shown from ground-based Fourier-transform infrared (FTIR) spectrometers and various satellite observations (Kohlhepp et al., 2011; Jones et al., 2011). When CFCs emission tends to be stable, HCl concentration in the upper stratosphere is dominated by the photochemical exposure which is also related to deep BDC (Waugh et al., 2007). However, the contrary HCl trends after 2006 in the mid-latitudes and the Arctic in boreal middle stratosphere (Fig. 2d and f) cannot be explained simply by the slowdown of the downwelling argued by Mahieu et al. (2014). There might be the opposite trends of the local downwelling in the mid-latitudes and the Arctic.

Therefore, the combination of variations of WV and HCl can be used to fully understand the change of deep BDC which is abbreviated as BDC in the below. Recent studies found that the BDC has weakened since the beginning of the 21st century in the Northern Hemisphere (NH) according to air age (Ploeger et al., 2015; Stiller et al., 2012). However, the mid-latitude air age in the middle and lower stratosphere is not only dominated by the deep BDC but also by the shallow BDC. Furthermore, the deep BDC and the shallow BDC can vary independently (Garny et al., 2011; Gerber, 2012; Stiller et al., 2012). Additionally, the HCl concentrations can be different in the air parcels with the same age but different transport pathways (Waugh et al., 2007). Therefore, the deep BDC has direct and efficient influence on the stratospheric HCl and WV. Hence, the mismatching trends of the WV in the tropics and HCl in the extratropics in the recent observations allow one to deduce an anomal latitudinal structural change in the BDC. This kind of latitudinal structure changes have not been discussed before.

Hence, we focused on two points in this study: (1) the latitudinal structure of the recent boreal BDC; (2) the connections between the latitudinal structure of the BDC changes and the mismatching trends of WV and HCl. The data set is described in Sect. 2. Section 3.1 and 3.2 present the trends of the boreal BDC and the latitudinal structural changes of the BDC. Section 3.3 shows the relationship between BDC and WV. Section 3.4 discusses the connection between BDC and HCl. The conclusion is provided in Sect. 4.

2 Data and methodology

2.1 Data

Monthly zonal average WV, HCl and temperature data are from Global OZone Chemistry And Related trace gas Data records for the Stratosphere (GOZCARDS Version 1.1) satellite data set. WV data is derived from Level 2 satellite products by HALOE (1991–2005) V19, UARS MLS (1991–1993) V5, ACE-FTS (2004–2012) V2.2 and Aura MLS (2004–2012) V3.3. HCl data is derived from Level 2 products by HALOE (1991–2005) V19, ACE-FTS (2004–2012) V2.2 and Aura MLS (2004–2012) V3.3. Temperature data is derived from MERRA (1979–2012) V5.2.0. Details can be obtained from http://gozcards.jpl.nasa.gov.

European Centre for Medium-Range Weather Forecast (ECMWF) ERA-Interim reanalysis monthly mean data (Dee et al., 2011) with $1.5^{\circ} \times 1.5^{\circ}$ grid was used to calculate Eliasen–Palm Flux (EPF) and Transformed Eulerian Mean (TEM) velocity.

ACPD
15, 24403–24417, 2015

2.2 Methodology

EPF of planetary waves (PWs, wave number 1–3) is expressed in Eq. (1) and TEM velocity (residual meridional circulation, approximative to BDC) is expressed in Eq. (2) (Andrews et al., 1987). In vector Figures of EPF, items are normalized by 3.14×6378 km horizontally and by 1000 hPa vertically. The unit is $m^2 s^{-2}$ (http://www.esrl.noaa.gov/psd/data/epflux/).

$$\begin{cases} F_{(\varphi)} = -r_0 \cos\varphi \overline{u'v'} & \text{(1a)} \\ F_{(p)} = f r_0 \cos\varphi \dfrac{\overline{v'\theta'}}{\overline{\theta}_p} & \text{(1b)} \end{cases}$$

$$\begin{cases} \overline{v}^* = \overline{v} - \dfrac{\partial}{\partial p}\left(\dfrac{\overline{v'\theta'}}{\overline{\theta}_p}\right) & \text{(2a)} \\ \overline{\omega}^* = \overline{\omega} + \dfrac{\partial}{r_0 \cos\varphi \partial\varphi}\left(\dfrac{\overline{v'\theta'}\cos\varphi}{\overline{\theta}_p}\right) & \text{(2b)} \end{cases}$$

Where overbars and primes denote zonal means and departures, subscripts without parentheses denote partial differentiation, p is the pressure, φ is the latitude, f is the Coriolis parameter, r_0 is the radius of the earth, θ is the potential temperature, u and v are zonal and meridional velocity, and ω is vertical velocity.

Deep BDC is driven by the breaking of PWs (EPF convergence) in the extratropical stratosphere in winter as known "downward-control principle" (Haynes et al., 1991; Holton et al., 1995). Due to the vertical EPF expressed as Eq. (1b) (EPFp, the eddy heat flux) indicates the upward propagation of PWs mainly in extratropical stratosphere, EPFp in the lower stratosphere region 45–75° N could be a proxy for the BDC (Newman et al., 2001; Li and Thompson, 2013). Generally, EPFp is negative. Thus, absolute value of EPFp at 50 hPa in 45–75° N can represent the intensity of the BDC.

December–February (DJF) mean is used for boreal winter EPF, $\overline{\omega}^*$ and other dynamic variables. However, temperature is averaged from December to March (DJFM),

ACPD
15, 24403–24417, 2015

because the influence of PW activities in DJF on stratospheric temperature will continue till March (Newman et al., 2001).

After 25-month moving average, the high-frequency signals are eliminated, and long-term (more than two years) interannual variability is left. Linear regression is used to calculate the correlation between temperature and EPFp.

3 Results

3.1 Trends of the boreal BDC

The BDC proxy (EPFp at 50 hPa over 45–75° N in Fig. 1a) in DJF from ERA-Interim shows that BDC in boreal winter tended to increase in 1993–1999 period. However, the BDC proxy tends to weaken with a trend of $2.21 \times 10^5\,\mathrm{pa\,m^{-2}\,s^{-2}\,decade^{-1}}$ ($33\,\%\,\mathrm{decade}^{-1}$) after 2000, which passes statistical significance test at the 90 % confidence level. The change of upwelling in BDC can affect the tropical CPTT by dynamic heating. Thus, the tropical lowermost stratospheric temperature can test the long-term trend of BDC. During 2001–2011, the temperature near the tropical tropopause (10° S–10° N) (Fig. 1b) rises with a trend of $2.21\,\mathrm{K\,decade^{-1}}$ based on the GOZCARDS-MERRA data. The trend exceeds the significance test at the 99 % confidence level. The tropical tropopause warming is consistent with the declining of BDC observed in Fig. 1a. Apparently, the result is similar to the ozone analysis in the tropical lower stratosphere (Aschmann et al., 2014) that the BDC tends to decrease after 2000. In addition, the decline of BDC during 2001–2011 was confirmed by air age increases in the boreal main stratosphere from Lagrangian transport models and observations (Ploeger et al., 2015; Mahieu et al., 2014; Stiller et al., 2012).

3.2 The latitudinal structural changes of the BDC

There is not only a shift of the BDC trend but also latitudinal structural changes of the BDC after 2000. BDC (red thick hollow arrow in Fig. 1c) is a net Lagrangian transport of

ACPD
15, 24403–24417, 2015

mass through the middle atmosphere (Andrews and McIntyre, 1976). According to the principle of mass conservation, the flow would be accelerated if the flow pipe narrows. Figure 1f shows an acceleration of downwelling (also as shown by "downward black thin hollow arrow" in Fig. 1d and e) on the south side of axis of polar vertex (35–65° N in Fig. 1c) corresponding to the polar vortex enhancement (in Fig. 1d) at 20 hPa. 2007–2011 average TEM vertical speed of 4.02×10^{-4} pa s^{-1} increased by 24 % over 2001–2005 average TEM vertical speed of 3.25×10^{-4} pa s^{-1} (in Fig. 1f). Comparing to the averaged EPF (BDC proxy) and zonal wind in winter during the period of 2001–2011(Fig. 1c), the differences of EPF and zonal wind between 2007–2011 and 2001–2005 show that the decline in the upward propagation of PWs could result in a negative anomaly of BDC (red thick hollow arrows in Fig. 1d) accompanied by a polar vortex enhancement. It is suggested that the more powerful circumpolar westerly would block the downwelling brach of BDC outside the polar region. In other words, the downwelling branch narrowed equatorward and sank faster in the mid-latitudes (downward black thin hollow arrow in Fig. 1d). The regression of EPFp from Fig. 1a with temperature of DJFM in 2001–2011 (Fig. 1e) can also support the latitudinal structural changes during the period. A negative center (near −2 K) in the Arctic implies an upwelling anomaly (upward black thin hollow arrow) which is validated by the weakening downwelling and shifting to upwelling (in Fig. 1g) on the north side of axis of polar vertex (65–85° N) at 20 hPa. The anomalies of the temperature and TEM vertical velocity in the Arctic area indicate the downwelling branch was narrowing equatorward. The narrowing leads to a local speedup of downwelling in the mid-latitudes (Fig. 1f and the downward black thin hollow arrow in Fig. 1e) which is also verified by a positive center (near 0.5 K) in the middle stratosphere. The positive center (near 1.5 K in Fig. 1e accounts for 62 % of the total temperature increase in Fig. 1b) is located in the lowermost stratosphere over tropics, from which the reduction of the upwelling of BDC can be inferred (downward red thick hollow arrow).

To summarize, the reduction of the tropical upwelling and the local strengthening of the mid-latitude downwelling compose the latitudinal structural changes of the BDC

ACPD
15, 24403–24417, 2015

after 2000. The decline of upwelling is in accord with the BDC weakening. The local acceleration of the mid-latitude downwelling results from the branch narrowing equatorward which is related to weak planetary wave activity and cold polar vortex enhancement.

3.3 Relationship between BDC and WV

The decline of the upwelling branch controls the increase of the tropical lower stratospheric WV. According to "tape recorder" effect, the maximum warming 1.5 K (Fig. 1e) in tropical lowermost stratosphere, as caused by the decline of upwelling in the weakening BDC, results in an increase of the tropical lower stratospheric WV by dehydration of air crossing the cold-point tropical tropopause (Schiller et al., 2009) in 2001–2011. GOZCARDS data show that WV at 68 hPa in 2001–2011 increased by the linear rate of 0.60 ppmv decade^{-1} (17.5 % decade^{-1}) which exceeds the significance test at the 99 % confidence level (Fig. 2a). WV at 46 hPa showed a similar trend of 0.27 ppmv decade^{-1} (7.3 % decade^{-1}) that passes statistical significance test at the 90 % confidence level (Fig. 2b). Fueglistaler (2012) analyzed tropical stratospheric WV from HALOE and also found the trend after 2000.

3.4 Relationship between BDC and HCl

There is a trend shift of boreal HCl in 2006/07. GOZCARDS data at 32 hPa show that mid-latitude (40–60° N) stratospheric HCl had a decreasing trend at a linear rate −0.40 ppbv decade^{-1} (−25.5 % decade^{-1}) before 2006 and had an increasing trend of 0.38 ppbv decade^{-1} (24.7 % decade^{-1}) after 2006 (Fig. 2c). Both trends exceed the significance test at the 99 % confidence level. In order to show only the downwelling impacts, HCl regressed against the monthly solar 10.7 cm flux (at the 99 % confidence level) was removed from the monthly HCl data in Fig. 2d. Trend shift of the residual HCl remains in 2006/07. Trend after 2006 is 0.32 ppbv decade^{-1} and still passes statistical significance test at the 90 % confidence level. HCl in the mid-

ACPD
15, 24403–24417, 2015

latitudes had similar trends of -0.15 ppbv decade^{-1} (-11.3 % decade^{-1}) before 2006 and 0.33 ppbv decade^{-1} (24.5 % decade^{-1}) after 2006 at 46 hPa, -0.44 ppbv decade^{-1} (-24.8 % decade^{-1}) before 2006 and 0.17 ppbv decade^{-1} (9.8 % decade^{-1}) after 2006 at 22 hPa (pictures omitted), which was also noted by Mahieu et al. (2014). However, HCl in the Arctic (70–90° N) at 22 hPa continuously decreased after 2001 (Fig. 2e). Declining trend is -0.32 ppbv decade^{-1} which passes statistical significance test at the 95 % confidence level. After removal of the solar cycle signals (Fig. 2f), HCl reduced faster after 2006/07 which is opposite to that in the mid-latitudes. It is similar at 15 hPa in the Arctic (pictures omitted). According to the atmospheric continuity equation, mass flux determines the local HCl concentration. Under the approximate conditions of no divergence and no horizontal HCl gradient, the strength of the local downwelling dominates the extratropical lower stratospheric HCl concentration by downward transport. Therefore, the increase in the mid-latitudes and decrease in the Arctic of HCl after 2006/07 can support the local speedup in mid-latitude and slowdown in the Arctic of the downwelling resulting from the narrowing equatorward of the downwelling branch of BDC.

4 Conclusion and discussion

The trends of boreal BDC tended to decrease and create latitudinal structural changes after 2000. The latitudinal structure of recent changes in the boreal BDC presented the reduction of the tropical upwelling and the local strengthening of the mid-latitude downwelling. The acceleration of downwelling in the mid-latitudes is caused by the branch narrowing equatorward which is related to the weaker planetary wave activity and the stronger polar vortex. In addition, the variation of WV in the tropics and HCl in the extratropics support the latitudinal structural changes of the BDC. The increasing tropical lower stratospheric WV results from the higher tropical CPTT which is mainly caused by the decline of the upwelling after 2000. The increasing HCl in the mid-latitudes is caused by the local speedup of downwelling after 2006/07.

Numerous simulation studies (Eichelberger et al., 2005; Garcia and Randel, 2008; Butchart et al., 2010; Li et al., 2010; Fleming et al., 2011; Douglass et al., 2014) claimed that BDC will be stronger in the future. Those results are not consistent with the observations described in this paper. However, Winter and Bourqui (2011) found that mid-latitude zonal symmetric surface heating forcing, decreasing the meridional temperature gradient between the tropics and the mid-latitudes, results in a decline of the upward propagation of PWs in the polar region and enhances the polar vortex. Realistically, zonally asymmetric land-ocean warming is more likely to affect the PWs activity. Hu et al. (2014) confirmed that increasing the meridional temperature gradient of sea surface temperature (SST) could enhance the BDC and would be accompanied by increased PWs activity and a decline in the polar vortex. But in 2001–2011, the Pacific Decadal Oscillation (PDO) shifted from the warm phase to the cold phase. An increase of North Pacific SST weakened the meridional temperature gradient between the tropics and the mid-latitudes which was opposite to the simulation conditions of Hu et al. (2014). It appears the modification of the PDO in the meridional temperature gradient is a likely reason for the weaker PWs activity and the latitudinal structural changes in the boreal BDC in the beginning of the 21st century.

Acknowledgements. The provisions of online data by NASA and ECMWF are gratefully acknowledged. This study was supported by National Natural Science Foundation of China (Grant No. 41375047, 41305039, 91537213), China Scholarship Fund and Priority Academic Program Development of Jiangsu Higher Education Institutions (PAPD). This work was also partly supported by the National Oceanic and Atmospheric Administration (NOAA), National Environmental Satellite, Data and Information Service (NESDIS), Center for Satellite Applications and Research (STAR).

References

Andrews, D. G. and McIntyre, M. E.: Planetary waves in horizontal and vertical shear: the generalized Eliassen–Palm relation and the mean zonal acceleration, J. Atmos. Sci., 33, 2031–2048, 1976.

ACPD
15, 24403–24417, 2015

Andrews, D. G., Holton, J. R., and Leovy, C. B.: Middle Atmosphere Dynamics, Acad. Press Inc., New York, 481 pp., 1987.
Aschmann, J., Burrows, J. P., Gebhardt, C., Rozanov, A., Hommel, R., Weber, M., and Thompson, A. M.: On the hiatus in the acceleration of tropical upwelling since the beginning of the 21st century, Atmos. Chem. Phys., 14, 12803–12814, doi:10.5194/acp-14-12803-2014, 2014.
Bannister, R. N., O'Neill, A., Gregory, A. R., and Nissen, K. M.: The role of the south-east Asian monsoon and other seasonal features in creating the "tape-recorder" signal in the Unified Model, Q. J. Roy. Meteor. Soc., 130, 1531–1554, doi:10.1256/qj.03.106, 2004.
Bonazzola, M. and Haynes, P. H.: A trajectory-based study of the tropical tropopause region, J. Geophys. Res., 109, D20112, doi:10.1029/2003jd004356, 2004.
Dee, D. P., Uppala, S. M., Simmons, A. J., Berrisford, P., and Poli, P., Kobayashi, S., Andrae, U., Balmaseda, M. A., Balsamo, G., Bauer, P., Bechtold, P., Beljaars, A. C. M., van de Berg, L., Bidlot, J., Bormann, N., Delsol, C., Dragani, R., Fuentes, M., Geer, A. J., Haimberger, L., Healy, S. B., Hersbach, H., Hólm, E. V., Isaksen, L., Kållberg, P., Köhler, M., Matricardi, M., McNally, A. P., Monge-Sanz, B. M., Morcrette, J.-J., Park, B.-K., Peubey, C., de Rosnay, P., Tavolato, C., Thépaut, J.-N., and Vitart, F.: The ERA-Interim reanalysis: configuration and performance of the data assimilation system, Q. J. Roy. Meteor. Soc., 137, 553–597, doi:10.1002/qj.828, 2011.
Dessler, A. E., Schoeberl, M. R., Wang, T., Davis, S. M., Rosenlof, K. H., and Vernier, J. P.: Variations of stratospheric water vapor over the past three decades, J. Geophys. Res.-Atmos., 119, 12588–12598, doi:10.1002/2014JD021712, 2014.
Douglass, A. R., Strahan, S. E., Oman, L. D., and Stolarski, R. S.: Understanding differences in chemistry climate model projections of stratospheric ozone, J. Geophys. Res.-Atmos., 119, 4922–4939, doi:10.1002/2013JD021159, 2014.
Eichelberger, S. J. and Hartmann, D. L.: Changes in the strength of the Brewer–Dobson circulation in a simple AGCM, Geophys. Res. Lett., 32, L15807, doi:10.1029/2005GL022924, 2005.
Fleming, E. L., Jackman, C. H., Stolarski, R. S., and Douglass, A. R.: A model study of the impact of source gas changes on the stratosphere for 1850–2100, Atmos. Chem. Phys., 11, 8515–8541, doi:10.5194/acp-11-8515-2011, 2011.
Fueglistaler, S.: Stepwise changes in stratospheric water vapor?, J. Geophys. Res., 117, D13302, doi:10.1029/2012JD017582, 2012.

ACPD
15, 24403–24417, 2015

Garcia, R. R. and Randel, W. J.: Acceleration of the Brewer–Dobson circulation due to increases in greenhouse gases, J. Atmos. Sci, 65, 2731–2739, doi:10.1175/2008JAS2712.1, 2008.

Garny, H., Dameris, M., Randel, W., Bodeker, G. E., and Deckert, R.: Dynamically forced increase of tropical upwelling in the lower stratosphere, J. Atmos. Sci., 68, 1214–1233, doi:10.1175/2011JAS3701.1, 2011.

Geller, M. A., Zhou, X. L., and Zhang, M. H.: Simulations of the interannual variability of stratospheric water vapor, J. Atmos. Sci., 59, 1076–1085, doi:10.1175/1520-0469(2002)059<1076:SOTIVO>2.0.CO;2, 2002.

Gerber, E. P.: Stratospheric versus tropospheric control of the strength and structure of the Brewer–Dobson circulation, J. Atmos. Sci., 69, 2857–2877, doi:10.1175/JAS-D-11-0341.1, 2012.

Haynes, P. H., McIntyre, M. E., Shepherd, T. G., Marks, C. J., and Shine, K. P.: On the "downward control" of extratropi cal diabatic circulations by eddy induced mean zonal forces, J. Atmos. Sci., 48, 651–678, doi:10.1175/1520-0469(1991)048<0651:OTCOED>2.0.CO;2, 1991.

Holton, J. R., Haynes, P. H., McIntyre, M. E., Douglas, A. R., Rood, R. B., and Pfister, L.: Stratosphere–troposphere exchange, Rev. Geophys., 33, 403–439, doi:10.1029/95RG02097, 1995.

Hu, D., Tian, W., Xie, F., Shu, J., and Dhomse, S.: Effects of meridional sea surface temperature changes on stratospheric temperature and circulation, Adv. Atmos. Sci., 31, 888–900, 2014.

Jones, A., Urban, J., Murtagh, D. P., Sanchez, C., Walker, K. A., Livesey, N. J., Froidevaux, L., and Santee, M. L.: Analysis of HCl and ClO time series in the upper stratosphere using satellite data sets, Atmos. Chem. Phys., 11, 5321–5333, doi:10.5194/acp-11-5321-2011, 2011.

Kohlhepp, R., Barthlott, S., Blumenstock, T., Hase, F., Kaiser, I., Raffalski, U., and Ruhnke, R.: Trends of HCl, $ClONO_2$, and HF column abundances from ground-based FTIR measurements in Kiruna (Sweden) in comparison with KASIMA model calculations, Atmos. Chem. Phys., 11, 4669–4677, doi:10.5194/acp-11-4669-2011, 2011.

Li, F., Stolarski, R. S., Pawson, S., Newman, P. A., and Waugh, D.: Narrowing of the upwelling branch of the Brewer–Dobson circulation and Hadley cell in chemistry-climate model simulations of the 21st century, Geophys. Res. Lett., 37, L13702, doi:10.1029/2010GL043718, 2010.

ACPD
15, 24403–24417, 2015

Title Page
Abstract | Introduction
Conclusions | References
Tables | Figures
◀▌ | ▶▌
◀ | ▶
Back | Close
Full Screen / Esc
Printer-friendly Version
Interactive Discussion

Li, Y. and Thompson, D. W. J.: The signature of the stratospheric Brewer–Dobson circulation in tropospheric clouds, J. Geophys. Res.-Atmos., 118, 3486–3494, doi:10.1002/jgrd.50339, 2013.

Mahieu, E., Chipperfield, M. P., Notholt, J., Reddmann, T., Anderson, J., Bernath, P. F., Blumenstock, T., Coffey, M. T., Dhomse, S. S., Feng, W., Franco, B., Froidevaux, L., Griffith, D. W. T., Hannigan, J. W., Hase, F., Hossaini, R., Jones, N. B., Morino, I., Murata, I., Nakajima, H., Palm, M., Paton-Walsh, C., Russell III, J. M., Schneider, M., Servais, C., Smale D., and Walker, K. A.: Recent Northern Hemisphere stratospheric HCl increase due to atmospheric circulation changes, Nature, 515, 104–107, doi:10.1038/nature13857, 2014.

Mohanakumar, K.: Stratosphere Troposphere Interactions, Springer Press, Milton Keynes, UK, 416 pp., 2008.

Mote, P. W., Rosenlof, K. H., Holton, J. R., Harwood, R. S., and Waters, J. W.: Seasonal-variations of water-vapor in the tropical lower stratosphere, Geophys. Res. Lett., 22, 1093–1096, doi:10.1029/95gl01234, 1995.

Newman, P. A., Nash, E. R., and Rosenfield, J. E.: What controls the temperature of the Arctic stratosphere during the spring?, J. Geophys. Res., 106, 19999–20010, doi:10.1029/2000JD000061, 2001.

Ploeger, F., Riese, M., Haenel, F., Konopka, P., Muller, R., and Stiller, G.: Variability of stratospheric mean age of air and of the local effects of residual circulation and eddy mixing, J. Geophys. Res.-Atmos., 120, 716–733, doi:10.1002/2014JD022468, 2015.

Schiller, C., Grooß, J.-U., Konopka, P., Plöger, F., Silva dos Santos, F. H., and Spelten, N.: Hydration and dehydration at the tropical tropopause, Atmos. Chem. Phys., 9, 9647–9660, doi:10.5194/acp-9-9647-2009, 2009.

Solomon, S., Rosenlof, K. H., Portmann, R. W., Daniel, J. S., Davis, S. M., Sanford, T. J., and Plattner, G. K.: Contributions of stratospheric water vapor to decadal changes in the rate of global warming, Science, 327, 1219–1223, doi:10.1126/science.1182488, 2010.

Stiller, G. P., von Clarmann, T., Haenel, F., Funke, B., Glatthor, N., Grabowski, U., Kellmann, S., Kiefer, M., Linden, A., Lossow, S., and López-Puertas, M.: Observed temporal evolution of global mean age of stratospheric air for the 2002 to 2010 period, Atmos. Chem. Phys., 12, 3311–3331, doi:10.5194/acp-12-3311-2012, 2012.

Winter, B. and Bourqui, M. S.: Sensitivity of the stratospheric circulation to the latitude of thermal surface forcing, J. Climate, 24, 5397–5415, doi:10.1175/2011JCLI4006.1, 2011.

ACPD
15, 24403–24417, 2015

The latitudinal structure of recent changes in the boreal Brewer–Dobson circulation

C. Shi et al.

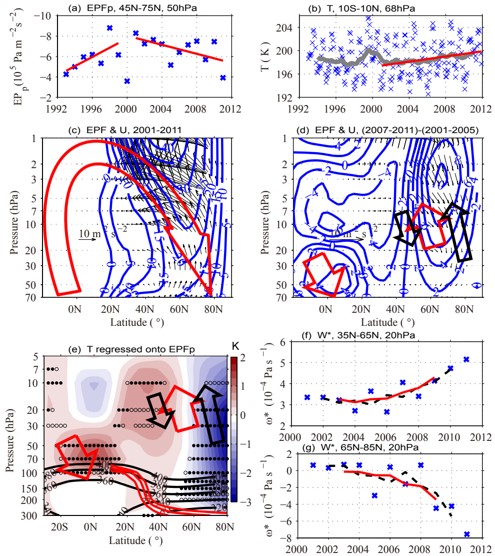

Figure 1. (a) Time series of 45–75° N mean vertical EPF of ERA-Interim in DJF at 50 hPa, thin lines for piecewise linear fitting; **(b)** 10° S–10° N mean monthly temperature from GOZCARDS in DJFM at 68 hPa, thin line for piecewise linear fitting and thick curve for 25-month running mean; **(c)** mean EPF (black thin arrows) of PW and zonal wind (contours, $\mathrm{m\,s^{-1}}$) in DJF of 2001–2011 from ERA-Interim, red thick hollow arrow indicate the deep branches of BDC; **(d)** as in **(c)**, but for the anomalies between 2007–2011 and 2001–2005, red thick hollow arrows indicate the anomalies of the deep BDC branch, black thin hollow arrows indicate the local anomalies in the weakening downwelling BDC branch; **(e)** temperature (in DJFM, unit, Kelvin) regressed on 45–75° N mean EPFp (in DJF at 50 hPa) in 2001–2011, Stippled regions passed the 90 % (filled) and 85 % (hollow) confidence test levels, black and red curves respectively indicate potential temperature and potential vorticity (2, 3, 4 PVU); **(f)** 35–65° N TEM vertical speed of BDC in DJF at 20 hPa, black and red curves respectively indicate 3 and 5 year running means; **(g)** as in **(f)**, but at 65–85° N.

ACPD
15, 24403–24417, 2015

Title Page
Abstract | Introduction
Conclusions | References
Tables | Figures
◄ | ►
◄ | ►
Back | Close
Full Screen / Esc
Printer-friendly Version
Interactive Discussion

ACPD
15, 24403–24417, 2015

The latitudinal structure of recent changes in the boreal Brewer–Dobson circulation

C. Shi et al.

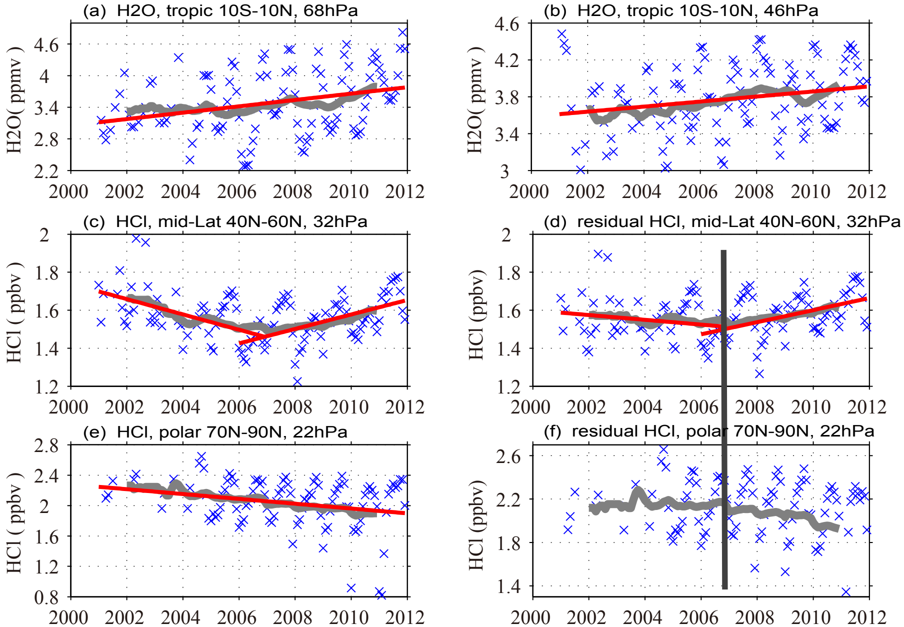

Figure 2. Time series of monthly H_2O and HCl from GOZCARDS, thick gray curve for 25-month running mean and thin red line for piecewise linear fitting; **(a, b)** H_2O in tropic 10° S–10° N at 68 and 46 hPa; **(c)** HCl in mid-latitude 40–60° N at 32 hPa; **(d)** as in **(c)**, but HCl regressed against the monthly solar 10.7 cm flux was removed from the results; **(e)** HCl in the Arctic 70–90° N at 22 hPa; **(f)** as in **(e)**, but HCl regressed against the monthly solar 10.7 cm flux was removed from the results.